iScience

CellPress
OPEN ACCESS

Article

The downregulation of IL-18R defines bona fide kidney-resident CD8$^+$ T cells

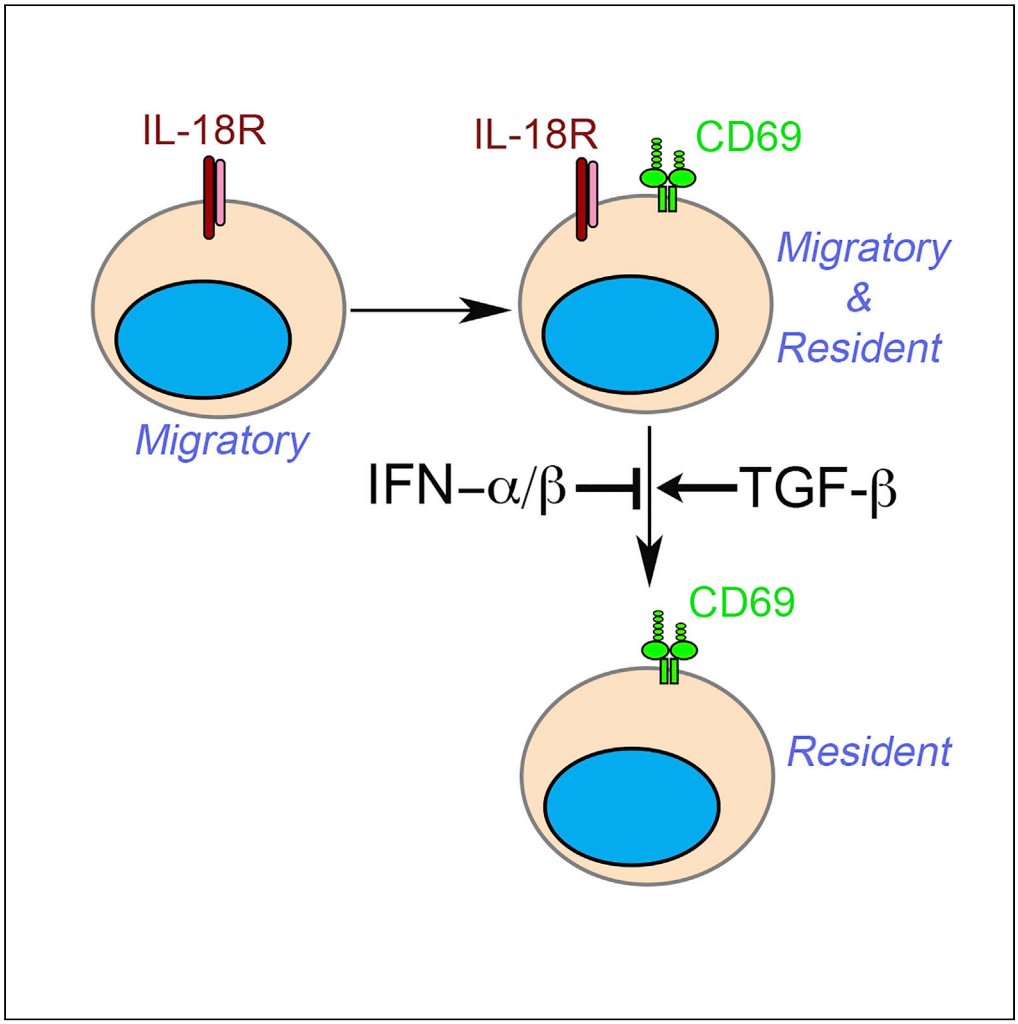

Wei Liao, Yong Liu, Chaoyu Ma, ..., Yuanzheng Qiu, Qianjin Lu, Nu Zhang

qianlu5860@gmail.com (Q.L.)
zhangn3@uthscsa.edu (N.Z.)

Highlights

CD8$^+$ Trm cells downregulate IL-18 receptor during differentiation

IL-18R^{hi} population is composed of both migratory and resident subsets

IL-18R^{lo} population is exclusively tissue-resident

TGF-β promotes, whereas IFN-α/β inhibits, IL-18R downregulation

Liao et al., iScience *24*, 101975
January 22, 2021 © 2020 The Author(s).
https://doi.org/10.1016/j.isci.2020.101975

iScience

CellPress
OPEN ACCESS

Article

The downregulation of IL-18R defines bona fide kidney-resident CD8$^+$ T cells

Wei Liao,[1,3,6] Yong Liu,[1,2,4,6] Chaoyu Ma,[1] Liwen Wang,[1,5] Guo Li,[1,2,4] Shruti Mishra,[1] Saranya Srinivasan,[1] Kenneth Ka-Ho Fan,[1] Haijing Wu,[3] Qianwen Li,[3] Ming Zhao,[3] Xun Liu,[1] Erika L. Demel,[1] Xin Zhang,[2,4] Yuanzheng Qiu,[2,4] Qianjin Lu,[3,*] and Nu Zhang[1,7,*]

Summary

Stepwise induction of CD69 and CD103 marks distinct differentiation stages of mucosal Trms. But the majority of non-mucosal Trm lacks CD103 expression. The expression of CD69 alone cannot faithfully define Trm cells in heavily vascularized non-mucosal tissues, such as the kidney. Here, we found that a subset of kidney Trms downregulated IL-18 receptor during differentiation. Via global transcriptional analysis and parabiosis experiments, we have discovered that the downregulation of interleukin-18 receptor (IL-18R) is associated with the establishment of tissue residency. Together with the expression of CD69, IL-18R^{lo} exclusively identify tissue-resident cells whereas IL-18R^{hi} population contains both tissue-resident and migratory ones. Local cytokines including transforming growth factor β (TGF-β) and interferon α (IFN-α)/β as well as TGF-β-dependent suppression of transcription factor Tcf-1 are essential for IL-18R downregulation during kidney Trm differentiation. Together, we identified a convenient surface marker to distinguish bona fide kidney-resident CD8$^+$ T cells as well as underlying molecular mechanisms controlling this differentiation process.

Introduction

Tissue-resident memory T (Trm) cells represent a distinct memory T cell population that is separated from the circulation and provides immediate protection against local reinfection (Cauley and Lefrancois, 2013; Clark, 2015; Iijima and Iwasaki, 2015; Mueller et al., 2013; Mueller and Mackay, 2016; Park and Kupper, 2015; Schenkel and Masopust, 2014; Thome and Farber, 2015). With variable accuracy, only a handful of surface markers, including CD69 and CD103, have been established to distinguish Trms from circulating T cells. The two-step differentiation model has been proposed for skin Trms (Mackay et al., 2013). After exiting bloodstream, effector CD8$^+$ T cells induce CD69 expression as the first step followed by the acquisition of CD103 as the second step. It is generally accepted that CD103^{hi} phenotype is tightly linked with the establishment of tissue residency and the loss of migratory capacity. However, the expression of CD103 is largely restricted to mucosal or barrier tissues, such as the intestines, skin, salivary glands, and lung. The vast majority of non-mucosal Trms do not express CD103 (Steinert et al., 2015). Whether CD69$^+$ Trms within a non-mucosal tissue represent a homogeneous or heterogeneous cell population remains unknown. Because the upregulation of CD69 on Trm precursors is a very early event, whether additional differentiation steps exist after the induction of CD69 remains unknown.

Because the expression of CD69 alone cannot accurately identify tissue resident T cells, intravascular labeling technique is widely used in Trm field to distinguish blood borne versus tissue-resident cells (Anderson et al., 2014). However, intravascular labeling can only provide localization information of a cell population at a given time (i.e., when intravascular labeling is performed). The results from intravascular labeling cannot tell the migratory history or migratory potential of a cell. Indeed, it has been reported that a blood-borne CD8$^+$ T cell can be a tissue-resident cell, especially in densely vascularized organs, such as the kidney (Steinert et al., 2015). It is unknown whether a cell surface marker exists to accurately identify bona fide tissue-resident T cells in the kidney.

[1]Department of Microbiology, Immunology and Molecular Genetics, Joe R. & Teresa Lozano Long School of Medicine, University of Texas Health Science Center at San Antonio, San Antonio, TX 78229, USA

[2]Department of Otolaryngology Head and Neck Surgery, Xiangya Hospital, Central South University, 87 Xiangya Road, Changsha, Hunan 410008, China

[3]Department of Dermatology, Hunan Key Laboratory of Medical Epigenomics, The Second Xiangya Hospital, Central South University, Changsha, Hunan 410011, China

[4]Otolaryngology Major Disease Research Key Laboratory of Hunan Province, 87 Xiangya Road, Changsha, Hunan 410008, China

[5]Department of Hematology, The Third Xiangya Hospital, Central South University, Changsha, Hunan 410013, China

[6]These authors contributed equally

[7]Lead contact

*Correspondence: qianlu5860@gmail.com (Q.L.), zhangn3@uthscsa.edu (N.Z.)

https://doi.org/10.1016/j.isci.2020.101975

This is an open access article under the CC BY-NC-ND license (http://creativecommons.org/licenses/by-nc-nd/4.0/).

Transforming growth factor β (TGF-β) is mainly involved in the acquisition of CD103 expression while dispensable for the initial induction of CD69 during Trm differentiation (Bergsbaken and Bevan, 2015; Thom et al., 2015). Even though TGF-β-independent induction of CD103 has been reported (Pizzolla et al., 2017), most previous research on TGF-β have been focused on $CD103^{hi}$ eTrm cells (i.e., Trm cells reside in the epithelial layers of barrier tissues) (Hu et al., 2015; Mackay et al., 2013; Mani et al., 2019; Sheridan et al., 2014; Zhang and Bevan, 2013). The function of TGF-β in non-barrier Trm differentiation remains less well defined.

Here, we discovered that kidney-resident $CD8^+$ T cells downregulated IL-18 receptor (IL-18R) after induction of CD69 during differentiation. Compared with IL-$18R^{hi}$ counterparts, IL-$18R^{lo}$ cells carried more common Trm signatures at transcription level. Via parabiosis experiments, we discovered that the downregulation of IL-18R was tightly associated with the establishment of kidney residency regardless of vascular location. TGF-β and suppression of transcription factor Tcf-1 (T cell factor-1) were required for IL-18R downregulation, whereas type I interferon (IFN) signals inhibited this process. Together, we have established IL-$18R^{lo}$ as a convenient surface marker to identify kidney-resident $CD8^+$ T cells as well as the molecular mechanisms controlling the downregulation of IL-18R.

Results

Kidney Trm downregulates IL-18 receptor

Mucosal Trm cells induce the expression of CD69 and CD103 in a progressive order, i.e., the induction of CD69 occurs usually before turning on CD103 (Mackay et al., 2013). The expression of CD103 is often associated with limited migratory capacity and tissue-resident phenotype. However, the expression of CD103 is usually not detectable or substantially delayed in non-mucosal and non-barrier tissues, such as the kidney (Casey et al., 2012). To investigate the differentiation of kidney-resident T cells, we employed the well-established LCMV (lymphocytic choriomeningitis virus) infection model. Briefly, congenically marked P14 TCR transgenic $CD8^+$ T cells specific for an LCMV epitope were adoptively transferred into unmanipulated C57BL/6 (B6) mice followed by acute LCMV Armstrong (LCMV Arm) infection (illustrated in Figure 1A). To distinguish blood-borne versus tissue-resident $CD8^+$ T cells, intra-vascular labeling of $CD8^+$ T cells was performed before euthanasia (Anderson et al., 2014). In both CD8α staining positive (intravascular, i.v.) and CD8α staining negative (extravascular, e.v.) compartments, a donor-derived P14 T cell population was clearly identified by congenic marker CD45.1 (Figure 1B). A subset of e.v. P14 T cells downregulated IL-18R after the induction of CD69. $CD69^+$ Trm cells could be further divided into two differentiation stages, namely IL-$18R^{hi}$ and IL-$18R^{lo}$ subsets (Figures 1B and 1C). There was a slight increase in the percentage of IL-$18R^{lo}$ subset at memory time points (e.g., day 42–62 in Figure 1D). Intriguingly, at a later memory time point (e.g., day 45), even though Trm cells were highly enriched in the e.v. compartment, we could consistently detect Trm-like cells ($CD69^+$IL-$18R^{hi}$ and $CD69^+$IL-$18R^{lo}$) in the i.v. compartment (Figures 1C and 1E). To be noted, compared with mucosal Trms (small intestine intraepithelial lymphocyte, SI-IEL) isolated from the same animals, we could not detect CD103 expression on kidney Trms (Figure 1F). Together, kidney Trm cells downregulate IL-18R during differentiation. Both IL-$18R^{hi}$ and IL-$18R^{lo}$ cells co-exist for a prolonged period of time in the kidney. Intravascular labeling cannot fully distinguish Trm versus non-Trm in the kidney, especially at later time points.

Downregulation of IL-18R is a common feature of Trms

Next, we investigated whether this phenomenon was kidney specific or not. To this end, we examined Trm cells isolated from salivary glands (SG) and SI-IEL of LCMV-infected animals. Both SG and SI-IEL Trms induce the expression of CD103 and downregulate circulating memory T cell marker Ly6C during differentiation. In both SG and SI-IEL, by first gating Trm cells based on their expression of IL-18R and CD69, it was clear that IL-$18R^{lo}$ Trms carried higher levels of CD103 and lower levels of Ly6C compared with their IL-$18R^{hi}$ counterparts (Figures 2A and 2B). Together, Trm cells downregulate IL-18R during differentiation, and IL-$18R^{lo}$ cells may represent a mature subset in both mucosal and non-mucosal tissues.

IL-18R is not required for Trm differentiation

To determine whether IL-18R signaling is involved in Trm differentiation or maturation, we generated congenically marked *Il18r1*$^{-/-}$ P14 TCR transgenic mice. As illustrated in Figure S1A, naive P14 T cells were isolated from both control and *Il18r1*$^{-/-}$ mice, mixed at a 1:1 ratio and adoptively co-transferred into B6 recipients followed by LCMV Arm infection. We examined Trm differentiation in both mucosal (SI-IEL) and non-mucosal tissues (kidney). In SI-IEL, we could not detect any significant changes in the

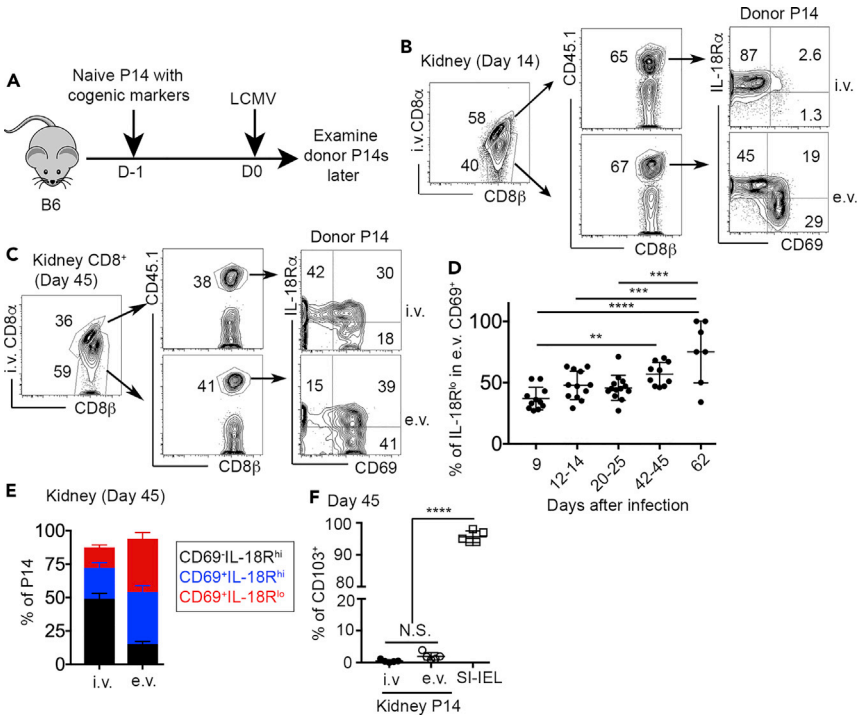

Figure 1. Downregulation of IL-18R during kidney Trm differentiation

(A) Experimental design. 10^4 congenically marked naive P14 T cells were transferred into B6 recipients followed by LCMV Arm infection on the next day.

(B and C) (B) Fourteen days after infection and (C) 45 days after infection, representative FACS profiles of kidney $CD8^+$ T cells are shown. (i.v., intravascular and e.v., extravascular).

(D) The percentage of $IL\text{-}18R^{lo}$ cells in e.v. $CD69^+$ P14 T cells.

(E) The composition of i.v. (left) versus e.v. (right) P14 T cells at day 45 post-infection.

(F) The percentage of $CD103^+$ cells in kidney P14s versus SI-IEL P14s at day 45. Pooled results from five independent experiments are shown in (D).

Representative results from two to three independent experiments are shown in (B), (C), (E), and (F). Each symbol in (D) and (F) represents the results from an individual mouse. **, $p < 0.01$; ***, $p < 0.001$; and ****, $p < 0.0001$ by one-way ANOVA with Tukey multi-comparison post-test. See also Figure S1. Bar graphs indicate the mean (±S.D.).

differentiation of $CD103^+$ Trms in *Il18r1*$^{-/-}$ cells, including the upregulation of CD73 and downregulation of Cmah (cytidine monophospho-N-acetylneuraminic acid hydroxylase) activities (Figures S1B and S1C). When focused on the kidney, we did not detect any significant defects in CD69 induction, Ly6C downregulation, or CD38 induction in both intravascular and extravascular compartments (Figures S1D–S1F). Therefore, we concluded that the lack of IL-18R did not impact Trm differentiation and maintenance, which was consistent with a previous report focused on intestinal Trm (Bergsbaken et al., 2017). In addition, we confirmed that in a different systemic viral infection model (Vesicular Stomatitis Virus), similar subsets of $CD69^+IL\text{-}18R^{hi}$ and $CD69^+IL\text{-}18R^{lo}$ kidney Trm cell can be identified (not depicted). Thus, even though IL-18 signaling is not required for the formation of Trms, the expression of IL-18R can be used as a biomarker to separate Trm cells into various differentiation stages.

Memory $CD8^+$ T cells exert effector functions in response to both antigen-specific and non-specific bystander stimulations. Cognate antigen induces robust activation of memory T cells, which represents the hallmark of immunological memory (Williams and Bevan, 2007). In the absence of cognate antigen, memory T cells rapidly produce inflammatory cytokines (e.g. IFN-γ) in response to type I IFN, IL-15, IL-12, and IL-18 (Berg et al., 2003; Berg and Forman, 2006; Kohlmeier et al., 2010; Kupz et al., 2012; Lauvau et al., 2016; Raue et al., 2013; Richer et al., 2015; Ruiz et al., 2014; Soudja et al., 2012). In contrast to type I IFN, IL-12, and IL-15, IL-18 is unique, as it is only required for bystander inflammatory responses without apparent involvement in antigen-elicited $CD8^+$ T cell responses (Haring and Harty, 2009). However, this conclusion about bystander response of memory $CD8^+$ T cells is almost exclusively based on the results

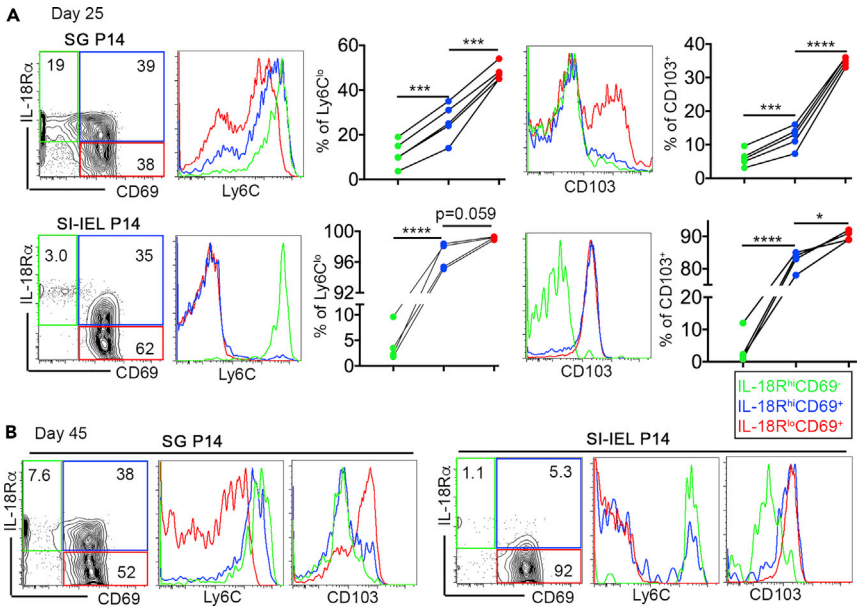

Figure 2. Downregulation of IL-18R during SG and SI-IEL Trm differentiation

Similar experimental setup to Figure 1. Day 25 (A) or day 45 (B) post-infection, SG P14 (upper row) and SI-IEL P14 (lower row) were isolated and subjected to flow cytometry analysis. Donor P14 T cells were first gated based on the expression of CD69 and IL-18R. The expression of Ly6C (left) and CD103 (right) on each subset were shown. Each group of connected symbols in (A) represents the results from an individual animal. *, $p < 0.05$; ***, $p < 0.001$; and ****, $p < 0.0001$ by one-way ANOVA with Tukey multi-comparison post-test. See also Figures S1 and S2.

from circulating cells residing in the secondary lymphoid organs. Whether Trm cells from non-lymphoid tissues respond to bystander inflammation in a similar manner as circulating memory T cells remains unclear. To probe the functional consequences of IL-18R downregulation during Trm differentiation, we examined their response to bystander inflammation. Because the large majority of SI-IEL Trms downregulate IL-18R at later time points (Figure 2B), we focused on SI-IEL Trms for this purpose. In contrast to splenic counterparts who responded to both cognate peptide (i.e., GP_{33-41} for P14 TCR) and bystander inflammation (i.e., IL-12+IL-18), SI-IEL Trm cells completely lost the response to bystander inflammation while maintaining the capacity to elicit a robust response to cognate antigen during *ex vivo* stimulation (Figure S2A). Using *Il18r1*$^{-/-}$ cells, we were able to demonstrate that the bystander response of splenic memory CD8$^+$ T cells was largely IL-18R dependent. In contrast, both WT and *Il18r1*$^{-/-}$ SI-IEL Trms could not respond to bystander stimuli (Figure S2B). Interestingly, TCR signal induced both IFN-γ and tumor necrosis factor (TNF) production, whereas bystander inflammatory cytokine only induced IFN-γ (Figure S2A), which is likely due to the fact that TNF production requires Ca^{2+} signaling (Falvo et al., 2010). Together, we propose that IL-18R downregulation in Trms may be related to the loss of response to IL-18-mediated bystander inflammation, which warrants future investigation.

Transcriptional and functional distinction of IL-18R^{hi} versus IL-18R^{lo} Trms

To further characterize IL-18R^{hi} and IL-18R^{lo} kidney T cells, we FACS sorted both populations as well as CD69$^-$ kidney P14 T cells and performed RNA-seq analysis. Taking advantage of published transcriptional signatures of both tissue-resident and circulating memory T cells (Mackay et al., 2013, 2016; Milner et al., 2017), we focused our analysis on these sets of resident and circulating signature genes. As shown in Figure 3A, for most circulating signature genes, their expression exhibited a steady decrease from CD69$^-$ and CD69$^+$IL-18R^{hi} to CD69$^+$IL-18R^{lo} populations. Conversely, a dramatic induction of the majority of resident signature genes occurred in CD69$^+$IL-18R^{lo} cells (Figure 3B).

In addition to IL-18Rα, several Trm-associated genes were differentially expressed at the protein level in CD69$^+$IL-18R^{hi} versus CD69$^+$IL-18R^{lo} kidney CD8$^+$ T cells (Figure 3C). The downregulation of Ly6C and Cmah activity were largely restricted to CD69$^+$IL-18R^{lo} cells. In contrast, the induction of CD38 and CXCR4 exhibited a stepwise increase during kidney Trm differentiation. Together, IL-18R^{hi} versus IL-18R^{lo}

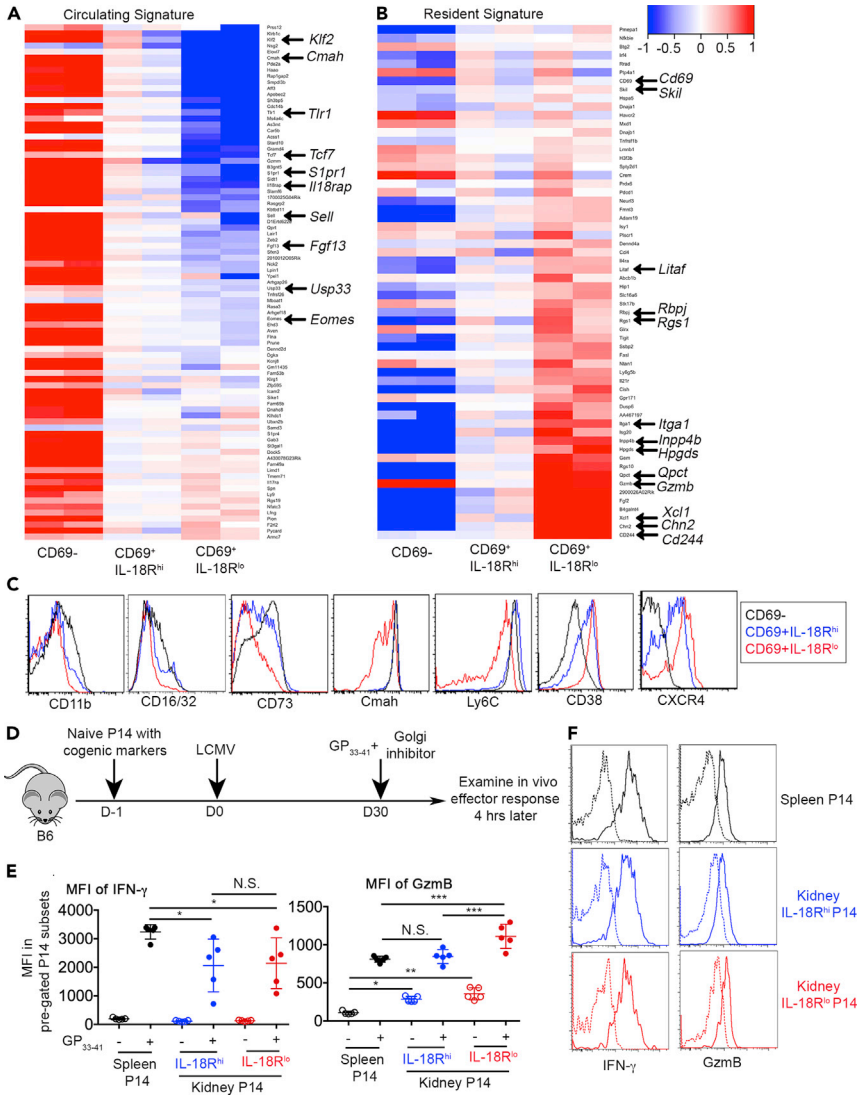

Figure 3. Transcriptional and functional distinction between IL-18R^{hi} and IL-18R^{lo} kidney Trms

Similar to Figure 1A, 12 days later, CD69^{-}, CD69^{+}IL-18R^{hi}, and CD69^{+}IL-18R^{lo} P14 T cells were FACS sorted from the kidney and subjected to RNA-seq analysis. The expression of (A) circulating signature genes and (B) resident signature genes are shown. Frequently identified Trm-associated genes are marked by arrows.

(C) Day 12–14 post-infection, kidney CD8^{+} T cells are pre-gated on CD69^{-}, CD69^{+}IL-18R^{hi}, and CD69^{+}IL-18R^{lo} cells, and the histograms of representative surface markers are shown. Each column in (A) and (B) represents a biologically independent replicate. Representative results from at least two independent experiments are shown in (C).

(D) Experimental design. Briefly, similar to Figure 1A, day 30 post-LCMV infection, the mice received GP$_{33-41}$ peptide via an intravenous route together with Brefeldin A. Mice were euthanized 4 h later.

(E) MFI of IFN-γ (left) and MFI of granzyme B (right) on pre-gated P14 subsets isolated from the spleen and kidney.

(F) Representative FACS profiles to show IFN-γ and granzyme B expression in kidney P14 subsets. Dotted lines, without GP$_{33-41}$; Solid lines, with GP$_{33-41}$.

Each symbol in (E) represents the results from an individual mouse. Representative results from two independent experiments are shown in (E). N.S., not significant, *, $p < 0.05$; **, $p < 0.01$; and ***, $p < 0.001$ by one-way ANOVA with Tukey multi-comparison post-test. See also Figure S3. Bar graphs indicate the mean (±S.D.).

cells represent distinct kidney-resident T cell subsets. Compared with IL-18R^{hi} ones, IL-18R^{lo} cells carry more common Trm signatures.

To probe whether Trm differentiation stages impact their effector function during recall responses, we stimulated P14 memory T cells with their cognate peptide *in vivo* and measured their effector molecule

production 4 h later before massive proliferation or before recruitment of circulating memory T cells occurred (illustrated in Figure 3D) (Beura et al., 2018; Park et al., 2018). To be noted, to avoid *ex vivo* incubation-induced confounding factors, cognate peptide and Golgi inhibitor were delivered *in vivo* and the production of effector molecules were measured on freshly isolated cells without further *in vitro* manipulation. As shown in Figure 3E left and Figure 3F, both IL-18R^{hi} and IL-18R^{lo} kidney Trm cells produced similar levels of IFN-γ upon re-stimulation. Consistent with recent findings that non-lymphoid tissue Trm cells are reactivated less efficiently than their lymphoid tissue counterparts (Low et al., 2020), both IL-18R^{hi} and IL-18R^{lo} Trms produced less IFN-γ than splenic memory T cells. Alternatively, this finding may be explained by inefficient access to cognate peptide for Trms *in vivo*. Indeed, when kidney Trms were isolated and stimulated *ex vivo* with peptide, we did not detect significant reduction of IFN-γ production (Figure S3). Different from IFN-γ, IL-18R^{lo} Trms produced significantly increased amount of granzyme B both at baseline and after re-stimulation (Figure 3E right and Figure 3F). In summary, compared with IL-18R^{hi} cells, IL-18R^{lo} Trms produce similar levels of IFN-γ and increased amounts of granzyme B upon reactivation *in vivo*.

IL-18R^{lo} Trm cells represent the bona fide tissue-resident population

To directly test the tissue residency of IL-18R^{hi} versus IL-18R^{lo} Trms, we performed parabiosis experiments. Briefly, B6 mice carrying P14 T cells with distinct congenic markers were surgically connected 30 days post-LCMV infection and examined 19–21 days later (Figure 4A). In the kidney, CD69^{+}IL-18R^{lo} subset was almost exclusively derived from the hosts. Interestingly, in both i.v. and e.v. compartments, CD69^{+}IL-18R^{lo} cells were similarly host-derived (Figures 4B and 4C). As expected, the vast majority of splenic P14 T cells were migratory and exhibited a roughly 50:50 ratio between host- and partner-derived cells, which was similar to CD69^{-}IL-18R^{hi} cells in the kidney. In contrast, SI-IEL compartment was mostly occupied by host-derived Trm cells (Figure 4C). For both i.v. and e.v. compartments, the transition from CD69^{+}IL-18R^{hi} to CD69^{+}IL-18R^{lo} stages was associated with significantly improved tissue-residency (Figure 4C). Importantly, using mucosal SI-IEL as a well-established Trm reference, the percentage of tissue residency was comparable among SI-IEL, kidney i.v. CD69^{+}IL-18R^{lo}, and e.v. CD69^{+}IL-18R^{lo} subsets (Figure 4C). These findings clearly demonstrate that the results from intravascular labeling does not tell the migratory history of a T cell. In stark contrast, the downregulation of IL-18R can be used as a convenient marker to faithfully define kidney-resident CD8^{+} T cells.

Because we have demonstrated that IL-18R^{lo} kidney-resident CD8^{+} T cells are formed at early stages after acute viral infection (i.e., day 12–14 post-infection, see Figures 1B and 1D), to further prove that IL-18R downregulation defines tissue residency even at these early stages, we performed another set of parabiosis experiments at an early time point (illustrated in Figure 4D). Briefly, B6 mice carrying P14 T cells with distinct congenic markers were surgically connected 12 days post-LCMV infection and examined 15 days later. As shown in Figure 4E, CD69^{+}IL-18R^{lo} kidney CD8^{+} T cells were exclusively derived from the hosts, indistinguishable from SI-IEL counterparts. In contrast, CD69^{+}IL-18R^{hi} cells contained a mixed population of both migratory and resident T cells.

Local cytokines control the downregulation of IL-18R in kidney Trms

Cytokine signals (e.g., IL-33, TNF and TGF-β) control the differentiation and maintenance of mucosal Trm cells (Bergsbaken et al., 2017; Hu et al., 2015; Mani et al., 2019; Skon et al., 2013; Slutter et al., 2017). To pinpoint the signals controlling IL-18R downregulation, we first used an *ex vivo* culture system. Day 4.5 post-infection when effector CD8^{+} T cells started to migrate from the secondary lymphoid organs to the periphery (Masopust et al., 2010), splenic P14 T cells were cultured overnight in the presence of a panel of different stimuli and the expression of IL-18R was measured. Both TCR and TGF-β significantly reduced the expression of IL-18R (Figure S4). IFN-β dramatically enhanced the expression of IL-18R, whereas IL-18, IL-33, and TNF did not yield significant changes (Figure S4). Based on this observation, we set up *in vivo* systems to investigate the involvement of TGF-β and type I IFN in the downregulation of IL-18R in kidney-resident CD8^{+} T cells.

TGF-β is specifically required for the downregulation of IL-18R during kidney Trm differentiation

TGF-β provides an essential signal for the induction of mucosal or epithelial Trm marker CD103 (El-Asady et al., 2005). Further, we have demonstrated that TGF-β promotes the formation of kidney Trms via enhancing effector CD8^{+} T cell extravasation at early stages (Ma et al., 2017). To investigate the possible roles of TGF-β in the downregulation of IL-18R during kidney Trm differentiation, we employed TGF-β

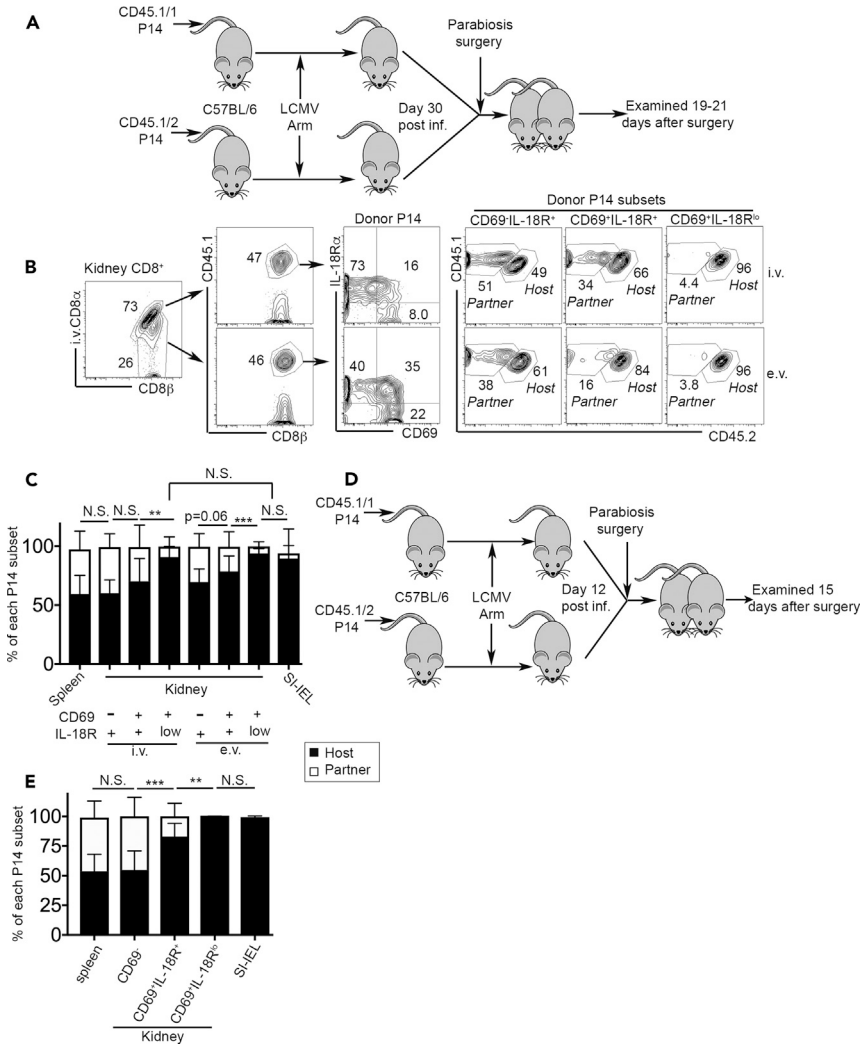

Figure 4. IL-18R^{lo} T cells represent a bona fide kidney-resident population

(A) Parabiosis experimental design for (B) to (D). Naive P14 T cells with distinct congenic markers were separately transferred into B6 mice followed by LCMV Arm infection. D30 p.i., pairs of mice carrying congenically different P14s were surgically connected and examined 19–21 days later.

(B) Representative FACS profiles of kidney CD8$^+$ T cells (n = 10).

(C) The composition (host- versus partner-derived) of each indicated P14 subset.

(D) Parabiosis experimental design for (E). D12 p.i., pairs of mice carrying congenically different P14s were surgically connected and examined 15 days later.

(E) Percentage of host-derived versus partner-derived cells within different P14 subsets are shown (n = 8).

Pooled results from two independent experiments are shown in (C) and (E). N.S., not significant, **, $p < 0.01$; ***, $p < 0.001$ by paired Student t test or one-way ANOVA with Tukey multi-comparison post-test. Bar graphs indicate the mean (±S.D.).

receptor conditional knockout (i.e., *Tgfbr2*$^{f/f}$dLck-cre (Zhang and Bevan, 2012), hereafter referred to as *Tgfbr2*$^{-/-}$) P14 T cells. Similar to the experimental design illustrated in Figure S1A, congenically marked naive control and *Tgfbr2*$^{-/-}$ P14 T cells were purified, mixed, and adoptively co-transferred into B6 recipients followed by LCMV infection. At day 14 post-infection, the percentage of CD69$^+$IL-18R^{hi} subset was comparable between control and *Tgfbr2*$^{-/-}$ P14 T cells (see blue numbers in Figure 5A), consistent with the results from the gut and salivary glands (Bergsbaken and Bevan, 2015; Thom et al., 2015). We did detect a slight but significant decrease of total number of CD69$^+$IL-18R^{hi} *Tgfbr2*$^{-/-}$ cells in the e.v. compartment (see blue symbols in Figure 5B), most likely due to defective extravasation of *Tgfbr2*$^{-/-}$ cells (Ma et al., 2017). However, the downregulation of IL-18R was significantly impaired in *Tgfbr2*$^{-/-}$ P14 T cells (see

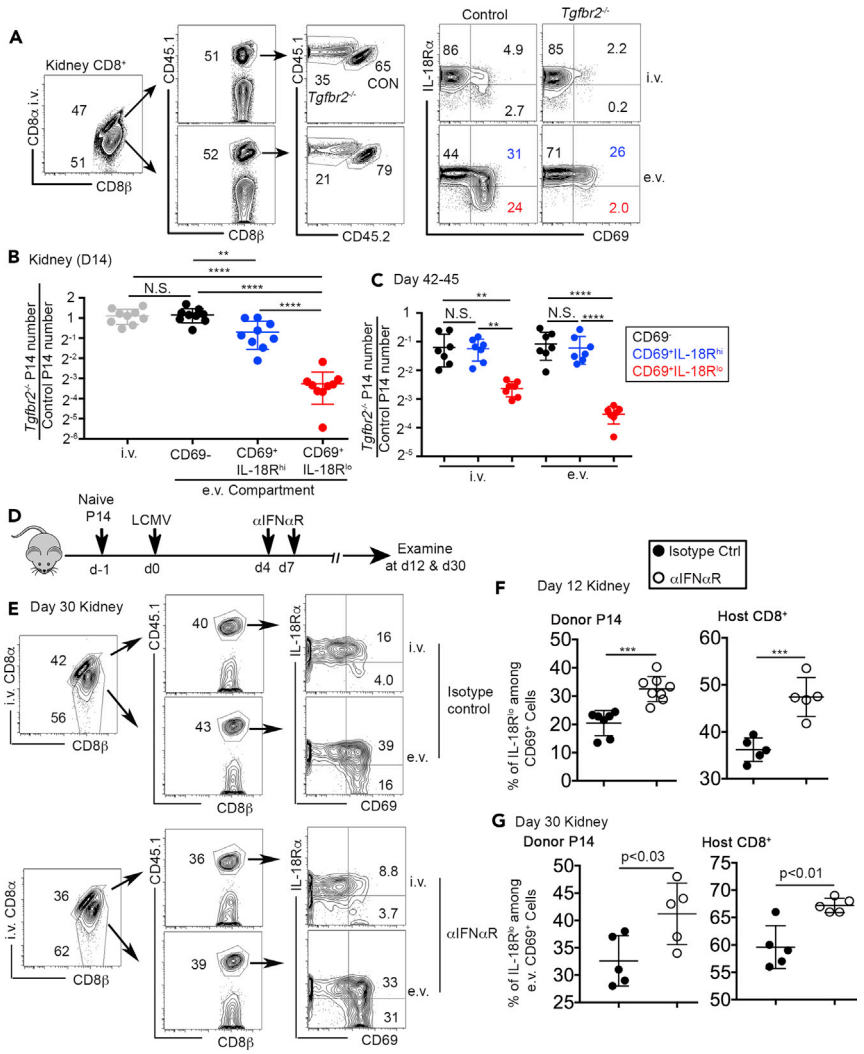

Figure 5. TGF-β and type I IFN control the downregulation of IL-18R during kidney Trm differentiation

Congenically marked control and *Tgfbr2*$^{-/-}$ P14 T cells were co-transferred into B6 mice followed by LCMV infection. Fourteen days post-infection, representative FACS profiles of pre-gated P14 T cells in both i.v. and e.v. compartments are shown in (A). (B) Day 14 and (C) day 42–45 post-infection, the ratio of (*Tgfbr2*$^{-/-}$ P14/Control P14) in each pre-gated kidney P14 subset. (D) Experimental design for (E) to (G). At day 4 and day 7 post-infection, 1 mg anti-IFNAR-1 or isotype control antibody was given i.p. Kidney P14 cells were examined later. (E) Day 30 post-infection, representative FACS profiles of kidney CD8$^+$ T cells. (F) Day 12 and (G) day 30 post-infection, the percentage of IL-18R^{lo} cells in donor P14 (left) or host CD8$^+$ T cells (right) in the kidney. Each symbol in (B), (C), (F), and (G) represents the results from an individual mouse. Pooled results from two to five independent experiments are shown in (B), (C), (F), and (G). N.S., not significant, **, $p < 0.01$, ***; $p < 0.001$; and ****, $p < 0.0001$ by Student t test or one-way ANOVA with Tukey multi-comparison post-test. See also Figures S4–S6. Bar graphs indicate the mean (±S.D.).

red numbers and symbols in Figures 5A and 5B). Further, this defect was not due to delayed downregulation of IL-18R in *Tgfbr2*$^{-/-}$ cells (Figure 5C). Importantly, at later time points (day 42–45) when there was a significant population of CD69$^+$ cells in the i.v. compartment of the kidney, we could clearly detect defective downregulation of IL-18R in *Tgfbr2*$^{-/-}$ P14 T cells isolated from both i.v. and e.v. compartments (Figure 5C), suggesting that TGF-β signal can be delivered to induce tissue-resident differentiation at both extravascular and intravascular sites. Furthermore, we performed another parabiosis experiment using WT and *Tgfbr2*$^{-/-}$ P14 T cells. Briefly, congenically distinct WT and *Tgfbr2*$^{-/-}$ P14 T cells were adoptively transferred into different B6 recipients followed by LCMV infection. Thirty days later, pairs of mice received WT, and *Tgfbr2*$^{-/-}$ P14 T cells were surgically connected. The distribution and differentiation of P14 T cells were examined 15 days after parabiosis surgery (Figure S5A). As shown in Figure S5B, only host-derived WT

control P14 T cells differentiated into IL-18R^{lo} kidney Trms, whereas *Tgfbr2*$^{-/-}$ P14 T cells exhibited indistinguishable differentiation patterns in host versus partner mice.

Here, we demonstrated that using the expression of IL-18R as a marker, CD69^{+} Trm cells could be further divided into two differentiation steps. Interestingly, TGF-β signaling is specifically required for the second step of Trm differentiation in the kidney, i.e., the downregulation of IL-18R after the induction of CD69. A similar scenario exists in mucosal or epithelial Trms, where TGF-β is only required for the induction of CD103 after acquiring CD69 (Bergsbaken and Bevan, 2015; Thom et al., 2015). Thus, TGF-β may represent the essential signal to Trm differentiation in both mucosal and non-mucosal tissues after establishing early residency.

Type I IFN inhibits IL-18R downregulation in kidney Trms

Next, we focused on type I IFNs, which provide the major inflammatory signal in our LCMV infection system. Interfering IFNα/β during the early stages of LCMV Arm infection (i.e., within the first 2–3 days) significantly impacted viral clearance and CD8^{+} T cell priming/expansion (not depicted (Cousens et al., 1999; Kolumam et al., 2005)). Further, effector CD8^{+} T cells usually leave secondary lymphoid organs and seed peripheral tissues around day 4 after LCMV Arm infection (Masopust et al., 2010). Thus, to avoid complications associated with early IFNα/β blocking and to specifically target Trm forming stages, we undertook a strategy illustrated in Figure 5D. Briefly, naive P14 T cells with congenic markers were adoptively transferred into B6 mice followed by LCMV infection. At day 4 and day 7 after infection, recipient mice were treated by anti-IFNAR1 blocking antibody or isotype control antibody. Trm cells were examined later. This type I IFN blocking strategy did not significantly alter the expansion or accumulation of P14 T cells in both secondary lymphoid and non-lymphoid tissues, including the kidney (Figure S6A) or effector CD8^{+} T cell differentiation in the spleen (Figure S6B). Importantly, we did not detect significant changes in viral clearance (Figure S6C). Consistent with previous findings that type I IFN was not required for the induction of CD69 on Trms *in vivo* (Mackay et al., 2015a), the expression of CD69 was largely intact (Figure 5E). In contrast, as shown in Figures 5E–5G, type I IFN blockade significantly enhanced the downregulation of IL-18R during kidney Trm differentiation. The enhanced downregulation of IL-18R can be detected as early as day 12 post-infection (Figure 5F). Interestingly, transient type I IFN blockade had a long-lasting effect on kidney-resident CD8^{+} T cells, as we could detect significant changes in kidney Trms at day 30 post-infection (Figures 5E and 5G). This result further supports the model that shortly after arrival at the kidney, CD8^{+} T cells acquire tissue residency under the influence of local signals. In addition, the effects of type I IFN were not restricted to monoclonal TCR transgenic P14 T cells; endogenous polyclonal kidney CD8^{+} T cells were also impacted in a similar manner (Figures 5F and 5G, right panels). Thus, inflammatory signal type I IFN negatively regulates the downregulation of IL-18R during kidney Trm differentiation.

Repression of transcription factor Tcf-1 is involved in the downregulation of IL-18R during Trm maturation

During Trm differentiation, TGF-β-mediated downregulation of T-box transcription factors T-bet and Eomes plays an essential role (Mackay et al., 2015b). To determine the transcription factors underlying TGF-β controlled Trm differentiation, we first focused on T-box transcription factors. However, neither *Tbx21* nor *Eomes* deficiency could rescue defective IL-18R downregulation in *Tgfbr2*$^{-/-}$ cells in the kidney (unpublished observations). Instead, consistent with our own RNA-seq results (Figure 3) and published RNA-seq results (Mackay et al., 2016; Milner et al., 2017), the expression of Tcf-1 (T cell factor-1, encoded by *Tcf7*) was suppressed during kidney Trm differentiation at the protein level (Figure 6A). Interestingly, compared with their WT control counterparts, both *Tgfbr2*$^{-/-}$ CD69^{+}IL-18R^{hi} and residual *Tgfbr2*$^{-/-}$ CD69^{+}IL-18R^{lo} cells expressed significantly higher levels of Tcf-1. To elucidate the function of Tcf-1 downregulation during Trm differentiation, we used a retroviral system to force express *Tcf7* in P14 T cells (Figure 6B). Consistent with published results of Tcf-1 in circulating effector and memory CD8^{+} T cells (Zhou et al., 2010), overexpression of *Tcf7* did not significantly impact the expansion of P14 T cells in the spleen, whereas the differentiation of KLRG-1^{-} memory precursors was enhanced and KLRG-1^{+} effector cells was inhibited (Figure S7). Compared with empty GFP control retrovirus, *Tcf7* overexpression significantly dampened the downregulation of IL-18R during kidney Trm differentiation at both early (day 14) and later (day 30) stages (Figures 6C–6E). At transcription level, suppression of Tcf-1 has been associated with Trm differentiation (Mackay et al., 2016; Milner et al., 2017). Recently, it has been reported that TGF-β-dependent downregulation of Tcf-1 is essential for lung-resident CD8^{+} T cell differentiation at functional level (Wu et al., 2020). Here, we showed that TGF-β suppressed the expression of Tcf-1, which may be essential for the downregulation of IL-18R associated with kidney Trm differentiation.

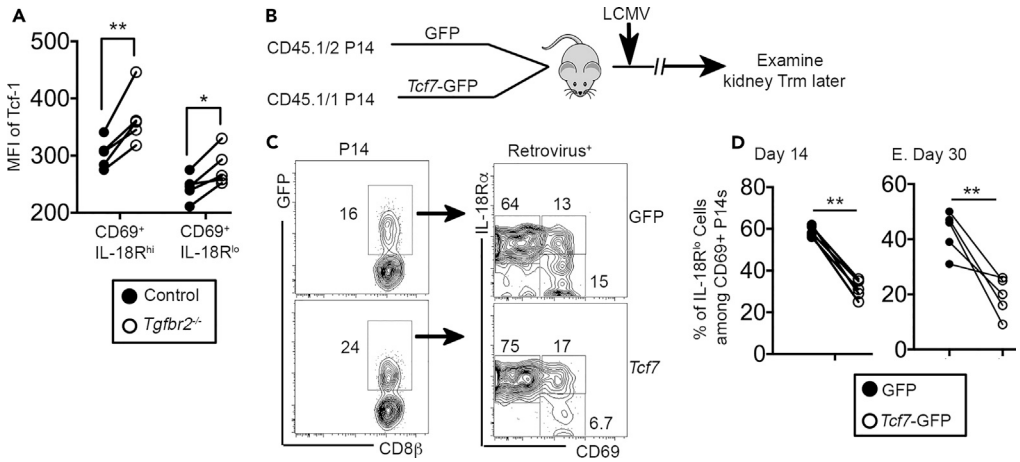

Figure 6. The downregulation of transcription factor Tcf-1 is required for IL-18R downregulation in the kidney

(A) Similar to the experimental setup in Figure 5A, day 14 post-LCMV infection, the expression of Tcf-1 was determined in pre-gated $CD69^+IL\text{-}18R^{hi}$ and $CD69^+IL\text{-}18R^{lo}$ kidney P14 T cells by flow cytometry.

(B) Experimental design. Activated P14 T cells were spin-infected by control retrovirus (GFP only) or retrovirus carrying *Tcf7* cDNA. One hour after spin infected, GFP-P14 and *Tcf7*-GFP-P14 were mixed and $2x10^5$ cells co-transferred into recipient B6 mice followed by LCMV infection. P14 T cells were examined later.

(C) Day 14 post-infection, representative FACS profiles of pre-gated kidney P14 T cells are shown.

(D and E) (D) Day 14 and (E) day 30 post-infection, the percentage of $IL\text{-}18R^{lo}$ cells in GFP^+CD69^+ P14 kidney T cells is shown. Each pair of symbols in (A), (D), and (E) represents the results from an individual recipient. Pooled results from two independent experiments are shown in (A), (D), and (E). *, $p < 0.05$ and **, $p < 0.01$ by paired Student t test. See also Figure S7.

Discussion

Together, we have analyzed Trm differentiation in the kidney and established that the downregulation of IL-18R is a distinct marker associated with the establishment of tissue residency. Further, this finding can be extended to other tissues, including SG and SI-IEL. As a convenient biomarker, $IL\text{-}18R^{lo}$ subset precisely indicates kidney residency regardless of its intra- or extra-vascular location. In contrast, $IL\text{-}18R^{hi}$ subset carries a mixture of tissue-resident and migratory T cells. TGF-β promotes, whereas type I IFN inhibits, the downregulation of IL-18R during kidney Trm differentiation. Further, the downregulation of transcription factor Tcf-1 is associated with this differentiation step of kidney Trms. Consistent with recent findings that reveal the heterogeneity of mucosal Trms (Kurd et al., 2020; Milner et al., 2020), our findings demonstrate that kidney $CD8^+$ T cells contain heterogeneous populations of cells with different levels of tissue residency.

Limitations of the study

In the current project, we focused on a systemic acute viral infection model and defined a differentiation process associated with $CD8^+$ tissue residency. Whether this finding could be extended to other infection models was not determined.

Resource availability

Lead contact

Further information and requests for resources and reagents should be directed to and will be fulfilled by the Lead Contact, Nu Zhang (zhangn3@uthscsa.edu)

Materials availability

This study did not generate new unique reagents.

Data and code availability

Original RNA-seq results can be accessed by GSE111801. The raw data supporting the current study are available from the Lead Contact upon request. All software is commercially available.

Methods

All methods can be found in the accompanying Transparent methods supplemental file.

Supplemental information

Supplemental information can be found online at https://doi.org/10.1016/j.isci.2020.101975.

Acknowledgments

We thank Dr. Tessa Bergsbaken (Rutgers New Jersey Medical School) and Dr. Linda Wakim (University of Melbourne, Australia) for critical reading of the manuscript, Dr. Haihui Xue (Hackensack University Medical Center) for providing Tcf7-GFP retroviral vector, and Dr. Linxi Li (University of Arkansas for Medical Sciences) for help with parabiosis experiments. This work is supported by NIH grants AI125701 and AI139721, Cancer Research Institute CLIP program, and American Cancer Society grant RSG-18-222-01-LIB to N.Z. and National Natural Science Foundation of China (No. 81522038, No. 81270024, and No. 81220108017) to Q.L. We thank Dr. Ben Daniel and Karla Gorena for FACS sorting. Flow Cytometry data was generated in the UT Health San Antonio Flow Cytometry Shared Resource Facility, which is supported in part by UT Health San Antonio, the Mays Cancer Center P30 Cancer Center Support Grant (NIH-NCI P30 CA054174) and the NIH National Center for Advancing Translational Sciences Clinical Translational Science Award (NIH-NCATS UL1 TR002645). We thank Drs. Zhao Lai, Yi Zou and Yidong Chen for RNA-seq analysis and informatics assistance. RNA-seq analysis was performed by the Genome Sequencing Core Facility at UTHSCSA, which is supported by NIH/NCI Cancer Center Support Grant P30 CA054174, NIH Shared Instrument grant 1S10OD021805-01, and Cancer Prevention and Research Institute of Texas (CPRIT) Core Facility grant RP160732. Special thanks to Dr. Rizi Ai (UCSD) for suggestions and help on bioinformatics.

Author contributions

Conceptualization, W.L., Y.L., Q.L., and N.Z.; Methodology, C.M. and X. L.; Investigation, W.L., Y.L., C.M., L.W., G.L., S.M., S.S., K.K-H.F., H.W., Q.L., M.Z., and E.L.D.; Writing–Original Draft, W.L., Q.L., X.Z., Y.Q., and N.Z.; Writing–Review & Editing, N.Z.; Supervision, Q.L. and N.Z.; Funding Acquisition, Q.L. and N.Z.

Declaration of interests

The authors declare no competing interests.

Received: July 24, 2020
Revised: December 1, 2020
Accepted: December 17, 2020
Published: January 22, 2021

References

Anderson, K.G., Mayer-Barber, K., Sung, H., Beura, L., James, B.R., Taylor, J.J., Qunaj, L., Griffith, T.S., Vezys, V., Barber, D.L., and Masopust, D. (2014). Intravascular staining for discrimination of vascular and tissue leukocytes. Nat. Protoc. *9*, 209–222.

Berg, R.E., Crossley, E., Murray, S., and Forman, J. (2003). Memory CD8+ T cells provide innate immune protection against Listeria monocytogenes in the absence of cognate antigen. J. Exp. Med. *198*, 1583–1593.

Berg, R.E., and Forman, J. (2006). The role of CD8 T cells in innate immunity and in antigen non-specific protection. Curr. Opin. Immunol. *18*, 338–343.

Bergsbaken, T., and Bevan, M.J. (2015). Proinflammatory microenvironments within the intestine regulate the differentiation of tissue-resident CD8(+) T cells responding to infection. Nat. Immunol. *16*, 406–414.

Bergsbaken, T., Bevan, M.J., and Fink, P.J. (2017). Local inflammatory cues regulate differentiation and persistence of CD8(+) tissue-resident memory T cells. Cell Rep. *19*, 114–124.

Beura, L.K., Mitchell, J.S., Thompson, E.A., Schenkel, J.M., Mohammed, J., Wijeyesinghe, S., Fonseca, R., Burbach, B.J., Hickman, H.D., Vezys, V., et al. (2018). Intravital mucosal imaging of CD8(+) resident memory T cells shows tissue-autonomous recall responses that amplify secondary memory. Nat. Immunol. *19*, 173–182.

Casey, K.A., Fraser, K.A., Schenkel, J.M., Moran, A., Abt, M.C., Beura, L.K., Lucas, P.J., Artis, D., Wherry, E.J., Hogquist, K., et al. (2012). Antigen-independent differentiation and maintenance of effector-like resident memory T cells in tissues. J. Immunol. *188*, 4866–4875.

Cauley, L.S., and Lefrancois, L. (2013). Guarding the perimeter: protection of the mucosa by tissue-resident memory T cells. Mucosal Immunol. *6*, 14–23.

Clark, R.A. (2015). Resident memory T cells in human health and disease. Sci. Transl. Med. *7*, 269rv261.

Cousens, L.P., Peterson, R., Hsu, S., Dorner, A., Altman, J.D., Ahmed, R., and Biron, C.A. (1999). Two roads diverged: interferon alpha/beta- and interleukin 12-mediated pathways in promoting T cell interferon gamma responses during viral infection. J. Exp. Med. *189*, 1315–1328.

El-Asady, R., Yuan, R., Liu, K., Wang, D., Gress, R.E., Lucas, P.J., Drachenberg, C.B., and Hadley, G.A. (2005). TGF-{beta}-dependent CD103 expression by CD8(+) T cells promotes selective destruction of the host intestinal epithelium during graft-versus-host disease. J. Exp. Med. *201*, 1647–1657.

Falvo, J.V., Tsytsykova, A.V., and Goldfeld, A.E. (2010). Transcriptional control of the TNF gene. Curr. Dir. Autoimmun. *11*, 27–60.

Haring, J.S., and Harty, J.T. (2009). Interleukin-18-related genes are induced during the contraction phase but do not play major roles in regulating the dynamics or function of the T-cell response to Listeria monocytogenes infection. Infect. Immun. *77*, 1894–1903.

Hu, Y., Lee, Y.T., Kaech, S.M., Garvy, B., and Cauley, L.S. (2015). Smad4 promotes differentiation of effector and circulating memory CD8 T cells but is dispensable for tissue-resident memory CD8 T cells. J. Immunol. *194*, 2407–2414.

Iijima, N., and Iwasaki, A. (2015). Tissue instruction for migration and retention of TRM cells. Trends Immunol. *36*, 556–564.

Kohlmeier, J.E., Cookenham, T., Roberts, A.D., Miller, S.C., and Woodland, D.L. (2010). Type I interferons regulate cytolytic activity of memory CD8(+) T cells in the lung airways during respiratory virus challenge. Immunity *33*, 96–105.

Kolumam, G.A., Thomas, S., Thompson, L.J., Sprent, J., and Murali-Krishna, K. (2005). Type I interferons act directly on CD8 T cells to allow clonal expansion and memory formation in response to viral infection. J. Exp. Med. *202*, 637–650.

Kupz, A., Guarda, G., Gebhardt, T., Sander, L.E., Short, K.R., Diavatopoulos, D.A., Wijburg, O.L., Cao, H., Waithman, J.C., Chen, W., et al. (2012). NLRC4 inflammasomes in dendritic cells regulate noncognate effector function by memory CD8(+) T cells. Nat. Immunol. *13*, 162–169.

Kurd, N.S., He, Z., Louis, T.L., Milner, J.J., Omilusik, K.D., Jin, W., Tsai, M.S., Widjaja, C.E., Kanbar, J.N., Olvera, J.G., et al. (2020). Early precursors and molecular determinants of tissue-resident memory CD8(+) T lymphocytes revealed by single-cell RNA sequencing. Sci. Immunol. *5*, eaaz6894.

Lauvau, G., Boutet, M., Williams, T.M., Chin, S.S., and Chorro, L. (2016). Memory CD8(+) T cells: innate-like sensors and orchestrators of protection. Trends Immunol. *37*, 375–385.

Low, J.S., Farsakoglu, Y., Amezcua Vesely, M.C., Sefik, E., Kelly, J.B., Harman, C.C.D., Jackson, R., Shyer, J.A., Jiang, X., Cauley, L.S., et al. (2020). Tissue-resident memory T cell reactivation by diverse antigen-presenting cells imparts distinct functional responses. J. Exp. Med. *217*, e20192291.

Ma, C., Mishra, S., Demel, E.L., Liu, Y., and Zhang, N. (2017). TGF-beta controls the formation of kidney-resident T cells via promoting effector T cell extravasation. J. Immunol. *198*, 749–756.

Mackay, L.K., Braun, A., Macleod, B.L., Collins, N., Tebartz, C., Bedoui, S., Carbone, F.R., and Gebhardt, T. (2015a). Cutting edge: CD69 interference with sphingosine-1-phosphate receptor function regulates peripheral T cell retention. J. Immunol. *194*, 2059–2063.

Mackay, L.K., Minnich, M., Kragten, N.A., Liao, Y., Nota, B., Seillet, C., Zaid, A., Man, K., Preston, S., Freestone, D., et al. (2016). Hobit and Blimp1 instruct a universal transcriptional program of tissue residency in lymphocytes. Science *352*, 459–463.

Mackay, L.K., Rahimpour, A., Ma, J.Z., Collins, N., Stock, A.T., Hafon, M.L., Vega-Ramos, J., Lauzurica, P., Mueller, S.N., Stefanovic, T., et al. (2013). The developmental pathway for CD103(+) CD8+ tissue-resident memory T cells of skin. Nat. Immunol. *14*, 1294–1301.

Mackay, L.K., Wynne-Jones, E., Freestone, D., Pellicci, D.G., Mielke, L.A., Newman, D.M., Braun, A., Masson, F., Kallies, A., Belz, G.T., and Carbone, F.R. (2015b). T-box transcription factors combine with the cytokines TGF-beta and IL-15 to control tissue-resident memory T cell fate. Immunity *43*, 1101–1111.

Mani, V., Bromley, S.K., Aijo, T., Mora-Buch, R., Carrizosa, E., Warner, R.D., Hamze, M., Sen, D.R., Chasse, A.Y., Lorant, A., et al. (2019). Migratory DCs activate TGF-beta to precondition naive CD8(+) T cells for tissue-resident memory fate. Science *366*, eaav5728.

Masopust, D., Choo, D., Vezys, V., Wherry, E.J., Duraiswamy, J., Akondy, R., Wang, J., Casey, K.A., Barber, D.L., Kawamura, K.S., et al. (2010). Dynamic T cell migration program provides resident memory within intestinal epithelium. J. Exp. Med. *207*, 553–564.

Milner, J.J., Toma, C., He, Z., Kurd, N.S., Nguyen, Q.P., McDonald, B., Quezada, L., Widjaja, C.E., Witherden, D.A., Crowl, J.T., et al. (2020). Heterogenous populations of tissue-resident CD8(+) T cells are generated in response to infection and malignancy. Immunity *52*, 808–824.e7.

Milner, J.J., Toma, C., Yu, B., Zhang, K., Omilusik, K., Phan, A.T., Wang, D., Getzler, A.J., Nguyen, T., Crotty, S., et al. (2017). Runx3 programs CD8(+) T cell residency in non-lymphoid tissues and tumours. Nature *552*, 253–257.

Mueller, S.N., Gebhardt, T., Carbone, F.R., and Heath, W.R. (2013). Memory T cell subsets, migration patterns, and tissue residence. Annu. Rev. Immunol. *31*, 137–161.

Mueller, S.N., and Mackay, L.K. (2016). Tissue-resident memory T cells: local specialists in immune defence. Nat. Rev. Immunol. *16*, 79–89.

Park, C.O., and Kupper, T.S. (2015). The emerging role of resident memory T cells in protective immunity and inflammatory disease. Nat. Med. *21*, 688–697.

Park, S.L., Zaid, A., Hor, J.L., Christo, S.N., Prier, J.E., Davies, B., Alexandre, Y.O., Gregory, J.L., Russell, T.A., Gebhardt, T., et al. (2018). Local proliferation maintains a stable pool of tissue-resident memory T cells after antiviral recall responses. Nat. Immunol. *19*, 183–191.

Pizzolla, A., Nguyen, T.H.O., Smith, J.M., Brooks, A.G., Kedzieska, K., Heath, W.R., Reading, P.C., and Wakim, L.M. (2017). Resident memory CD8(+) T cells in the upper respiratory tract prevent pulmonary influenza virus infection. Sci. Immunol. *2*, eaam6970.

Raue, H.P., Beadling, C., Haun, J., and Slifka, M.K. (2013). Cytokine-mediated programmed proliferation of virus-specific CD8(+) memory T cells. Immunity *38*, 131–139.

Richer, M.J., Pewe, L.L., Hancox, L.S., Hartwig, S.M., Varga, S.M., and Harty, J.T. (2015). Inflammatory IL-15 is required for optimal memory T cell responses. J. Clin. Invest. *125*, 3477–3490.

Ruiz, A.L., Soudja, S.M., Deceneux, C., Lauvau, G., and Marie, J.C. (2014). NK1.1+ CD8+ T cells escape TGF-beta control and contribute to early microbial pathogen response. Nat. Commun. *5*, 5150.

Schenkel, J.M., and Masopust, D. (2014). Tissue-resident memory T cells. Immunity *41*, 886–897.

Sheridan, B.S., Pham, Q.M., Lee, Y.T., Cauley, L.S., Puddington, L., and Lefrancois, L. (2014). Oral infection drives a distinct population of intestinal resident memory CD8(+) T cells with enhanced protective function. Immunity *40*, 747–757.

Skon, C.N., Lee, J.Y., Anderson, K.G., Masopust, D., Hogquist, K.A., and Jameson, S.C. (2013). Transcriptional downregulation of S1pr1 is required for the establishment of resident memory CD8+ T cells. Nat. Immunol. *14*, 1285–1293.

Slutter, B., Van Braeckel-Budimir, N., Abboud, G., Varga, S.M., Salek-Ardakani, S., and Harty, J.T. (2017). Dynamics of influenza-induced lung-resident memory T cells underlie waning heterosubtypic immunity. Sci. Immunol. *2*, eaag2031.

Soudja, S.M., Ruiz, A.L., Marie, J.C., and Lauvau, G. (2012). Inflammatory monocytes activate memory CD8(+) T and innate NK lymphocytes independent of cognate antigen during microbial pathogen invasion. Immunity *37*, 549–562.

Steinert, E.M., Schenkel, J.M., Fraser, K.A., Beura, L.K., Manlove, L.S., Igyarto, B.Z., Southern, P.J., and Masopust, D. (2015). Quantifying memory CD8 T cells reveals regionalization of immunosurveillance. Cell *161*, 737–749.

Thom, J.T., Weber, T.C., Walton, S.M., Torti, N., and Oxenius, A. (2015). The salivary gland acts as a sink for tissue-resident memory CD8(+) T cells, facilitating protection from local cytomegalovirus infection. Cell Rep. *13*, 1125–1136.

Thome, J.J., and Farber, D.L. (2015). Emerging concepts in tissue-resident T cells: lessons from humans. Trends Immunol. *36*, 428–435.

Williams, M.A., and Bevan, M.J. (2007). Effector and memory CTL differentiation. Annu. Rev. Immunol. *25*, 171–192.

Wu, J., Madi, A., Mieg, A., Hotz-Wagenblatt, A., Weisshaar, N., Ma, S., Mohr, K., Schlimbach, T., Hering, M., Borgers, H., and Cui, G. (2020). T cell factor 1 suppresses CD103+ lung tissue-resident memory T cell Development. Cell Rep *31*, 107484.

Zhang, N., and Bevan, M.J. (2012). TGF-beta signaling to T cells inhibits autoimmunity during lymphopenia-driven proliferation. Nat. Immunol. *13*, 667–673.

Zhang, N., and Bevan, M.J. (2013). Transforming growth factor-beta signaling controls the formation and maintenance of gut-resident memory T cells by regulating migration and retention. Immunity *39*, 687–696.

Zhou, X., Yu, S., Zhao, D.M., Harty, J.T., Badovinac, V.P., and Xue, H.H. (2010). Differentiation and persistence of memory CD8(+) T cells depend on T cell factor 1. Immunity *33*, 229–240.

iScience, Volume *24*

Supplemental Information

The downregulation of IL-18R defines bona fide kidney-resident $CD8^+$ T cells

Wei Liao, Yong Liu, Chaoyu Ma, Liwen Wang, Guo Li, Shruti Mishra, Saranya Srinivasan, Kenneth Ka-Ho Fan, Haijing Wu, Qianwen Li, Ming Zhao, Xun Liu, Erika L. Demel, Xin Zhang, Yuanzheng Qiu, Qianjin Lu, and Nu Zhang

Supplemental Figures

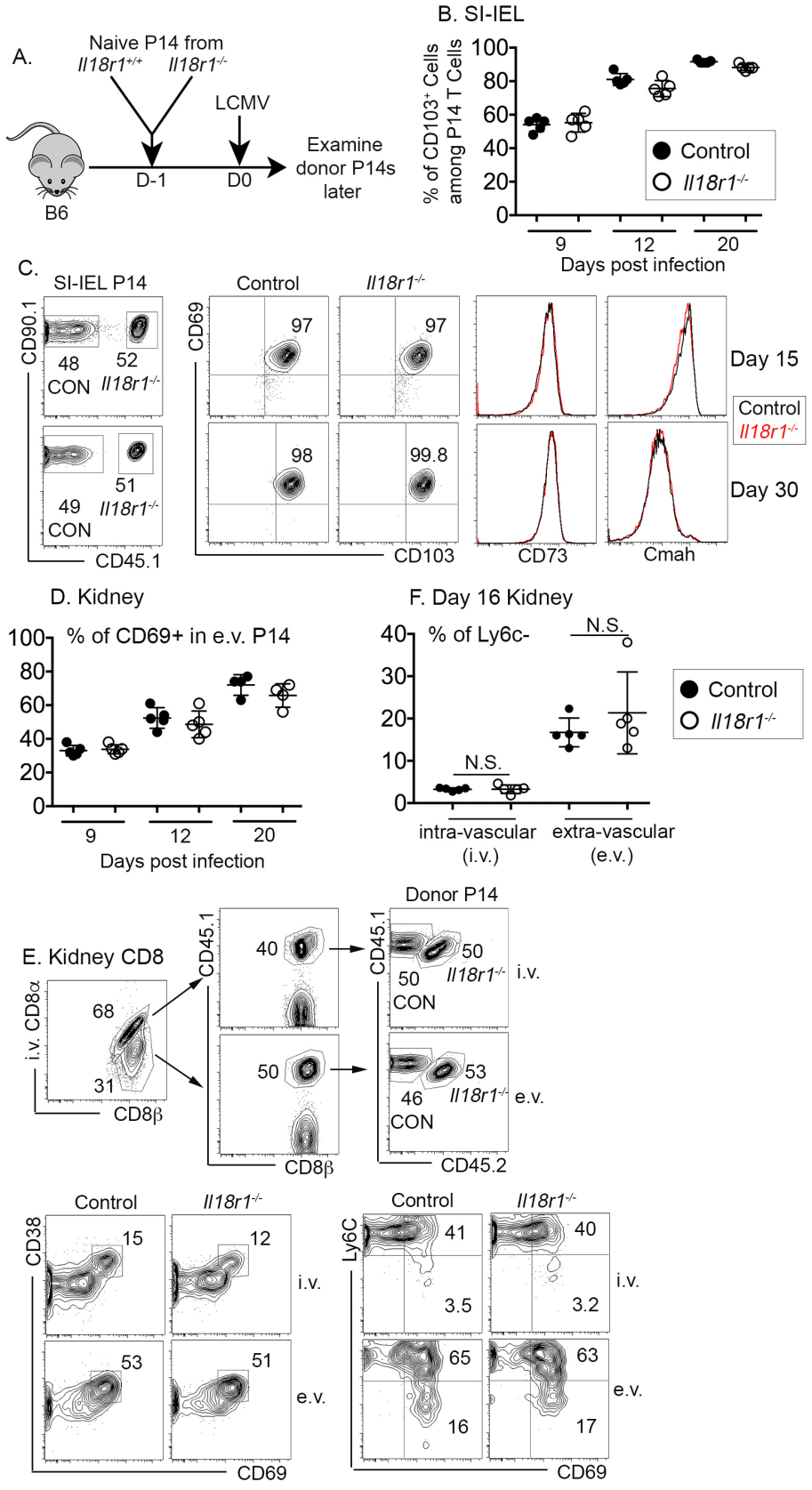

Figure S1. Apparently normal differentiation of Trms in the absence of IL-18R, Related to Figure 1 and Figure 2. (**A**) Experimental design. (**B**) At different time points after infection, the percentage of $CD69^{+}CD103^{+}$ cells among SI-IEL P14 T cells is shown. (**C**) Representative FACS profiles of SI-IEL P14 T cells at day 15 (upper) or day 30 (lower) after infection. (**D**) The percentage of $CD69^{+}$ cells among e.v. kidney P14 T cells is shown. (**E**) Representative FACS profiles of kidney P14 T cells at day 16 post infection. (**F**) The percentage of $Ly6C^{-}$ cells among indicated kidney P14 populations is shown. Each symbol in (**B**), (**D**) and (**F**) represents the results from an individual recipient mouse. Combined results from four independent experiments are shown. No statistical significance was detected at any time points between control and *Il18r1*$^{-/-}$ cells by Student *t*-test.

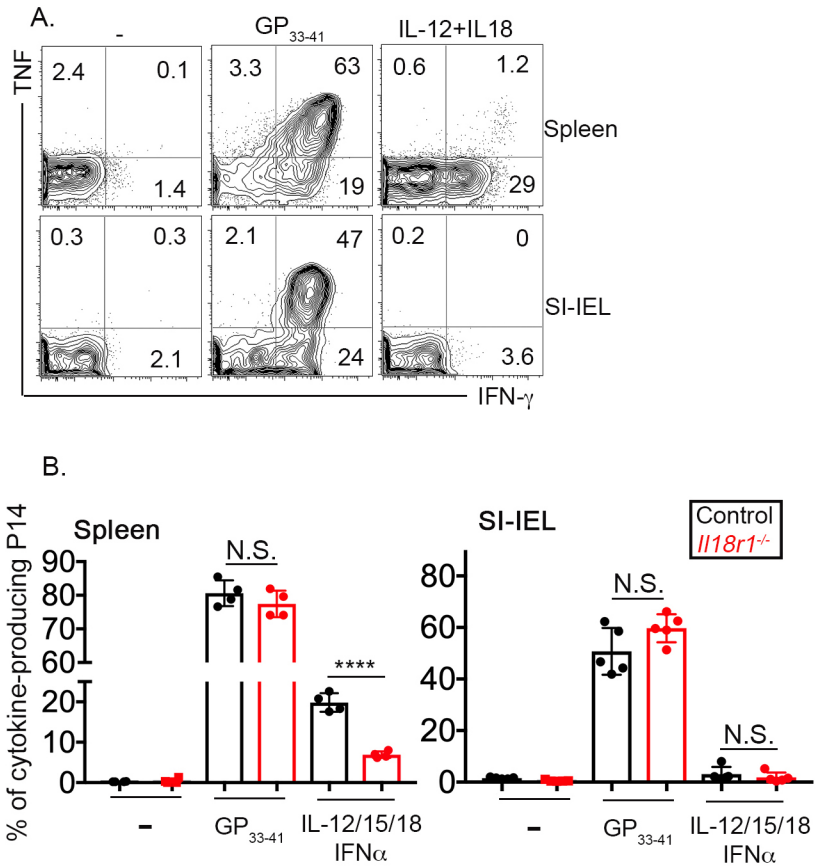

Figure S2. Downregulation of IL-18R is associated with the loss of response to bystander inflammation, Related to Figure 2. (**A**) Same experimental setup as in Figure 1 and 2. Day 30 post infection, splenic P14 and SI-IEL P14 were isolated and cultured for 4 hours ex vivo stimulation in the presence of Golgi STOP. Cytokine production was determined by intracellular FACS staining. Representative FACS profiles of pre-gated live P14 T cells are shown (n=5). (**B**) Same experimental setup as in Figure S1. Day 30 post infection, splenic and SI-IEL P14 were isolated and subjected to ex vivo stimulation and IFN-γ production was measured by intracellular FACS staining. Each symbol represents the results from an individual mouse. N.S., not significant and ****, p<0.0001 by Student *t*-test.

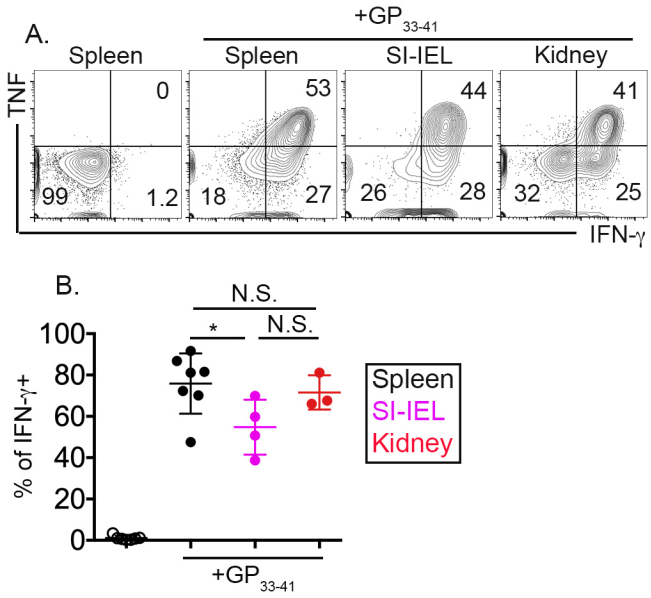

Figure S3. In vitro recall response of Trm, Related to Figure 3. Same experimental setup as in Figure 1. Day 30 post infection, P14 T cells were isolated and cultured with GP_{33-41} peptide in the presence of Golgi STOP for 4 hours. Cytokine production was measured by intracellular FACS staining. (**A**) Representative FACS profiles of pre-gated live P14 T cells are shown. (**B**) The percentage of IFN-γ^+ P14 T cells. Each symbol in (B) represents the results from an individual mouse. N.S., not significant and *, $p<0.05$ by One-way ANOVA with Tukey multi comparison post-test. Pooled results from 3 independent experiments are shown in (B).

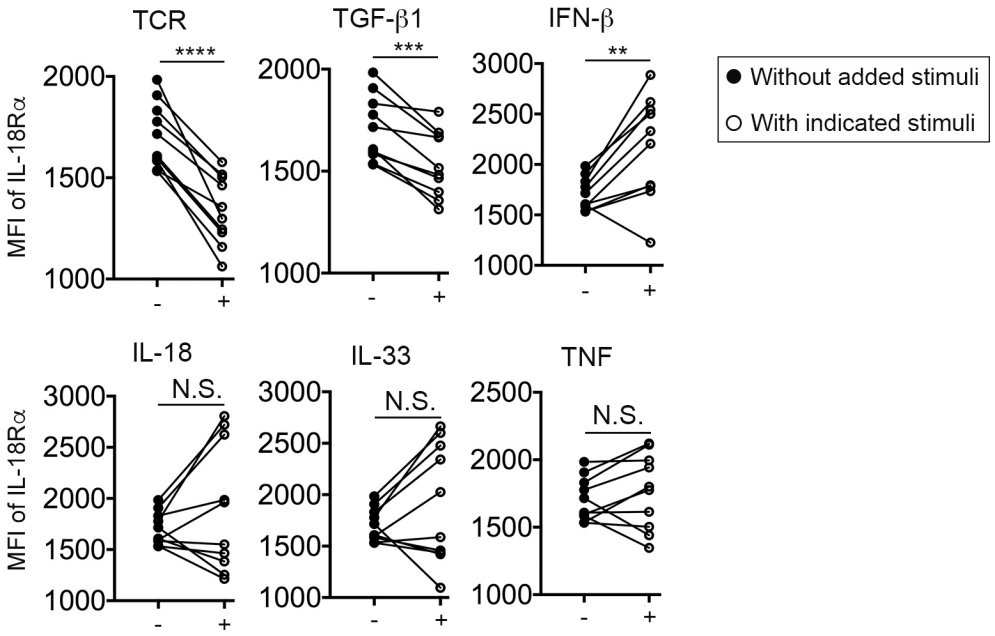

Figure S4. TGF-β and Type I IFN impact IL-18R expression of early effector T cells, Related to Figure 5. Naïve P14 T cells were adoptively transferred into B6 recipients followed by LCMV Arm infection. Day 4.5 post infection, splenic P14 T cells were isolated and cultured overnight with indicated stimuli: TCR (1μg/ml GP_{33-41}), 50ng/ml hTGF-β1, 20ng/ml IFN-β, 20ng/ml IL-18, 20ng/ml IL-33 and 20ng/ml TNF. All conditions include 5ng/ml IL-2 to keep effector T cell alive. MFI of IL-18Rα on live P14 T cells were measured by FACS. Each pairs of symbol represents the results from an individual recipient mouse. Pooled results from 3 independent experiments. N.S., not significant, **, $p<0.01$, ***, $p<0.001$ and ****, $p<0.0001$ by paired Student *t*-test.

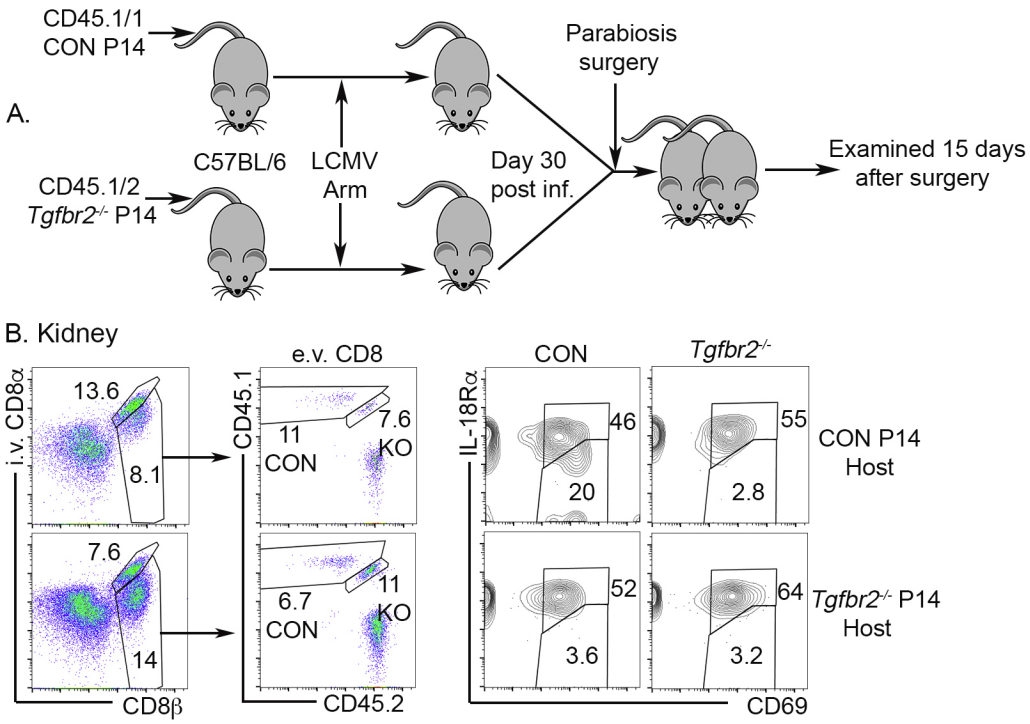

Figure S5. TGF-β is required for the differentiation of IL-18R^{lo} kidney-resident memory T cells, Related to Figure 5. (A) Experimental design. Naïve WT control and *Tgfbr2*$^{-/-}$ P14 T cells with distinct congenic markers were separately transferred into B6 mice followed by LCMV Arm infection. D30 p.i., pairs of mice carrying WT control and *Tgfbr2*$^{-/-}$ P14s were surgically connected and examined 15 days later. (**B**) Representative FACS profiles of kidney CD8^{+} T cells derived from the same parabiosis pair (n=4). Upper row, kidney sample from control P14 host; lower row, kidney sample from *Tgfbr2*$^{-/-}$ P14 host.

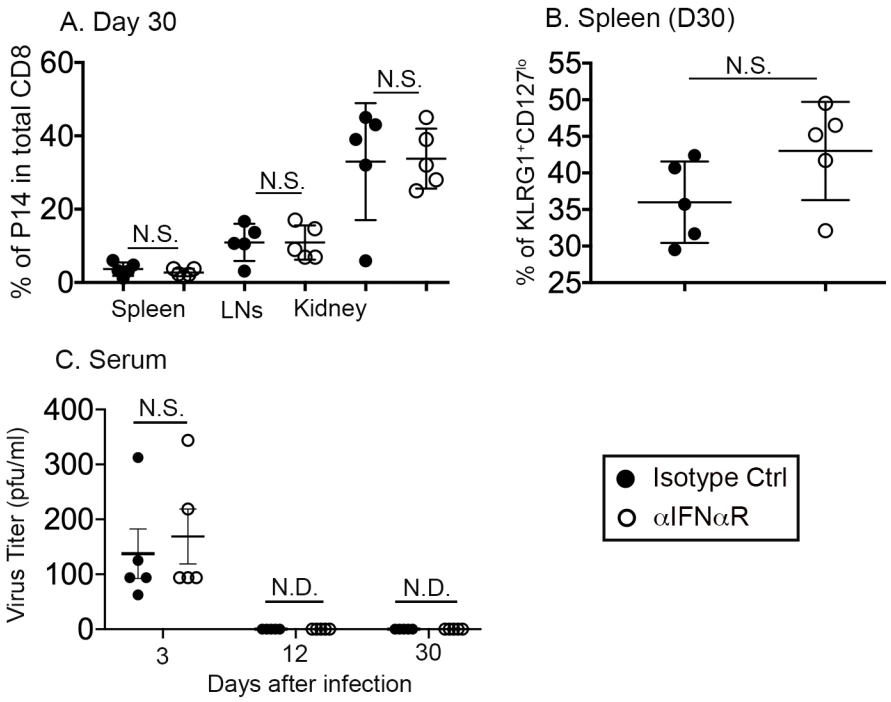

Figure S6. Type I IFN blockade at day 4 and day 7 does not impact CD8$^+$ T cell expansion and viral clearance, Related to Figure 5. Similar experimental setup to **Figure 5D**. (**A**) The percentage of donor P14 T cells in spleen, lymph nodes and kidney. (**B**) The percentage of KLRG1$^+$ cells in splenic P14. (**C**) Viral titer in the serum. Each symbol represents the results from an individual recipient. N.D., not detectable. N.S., not significant by Student *t*-test.

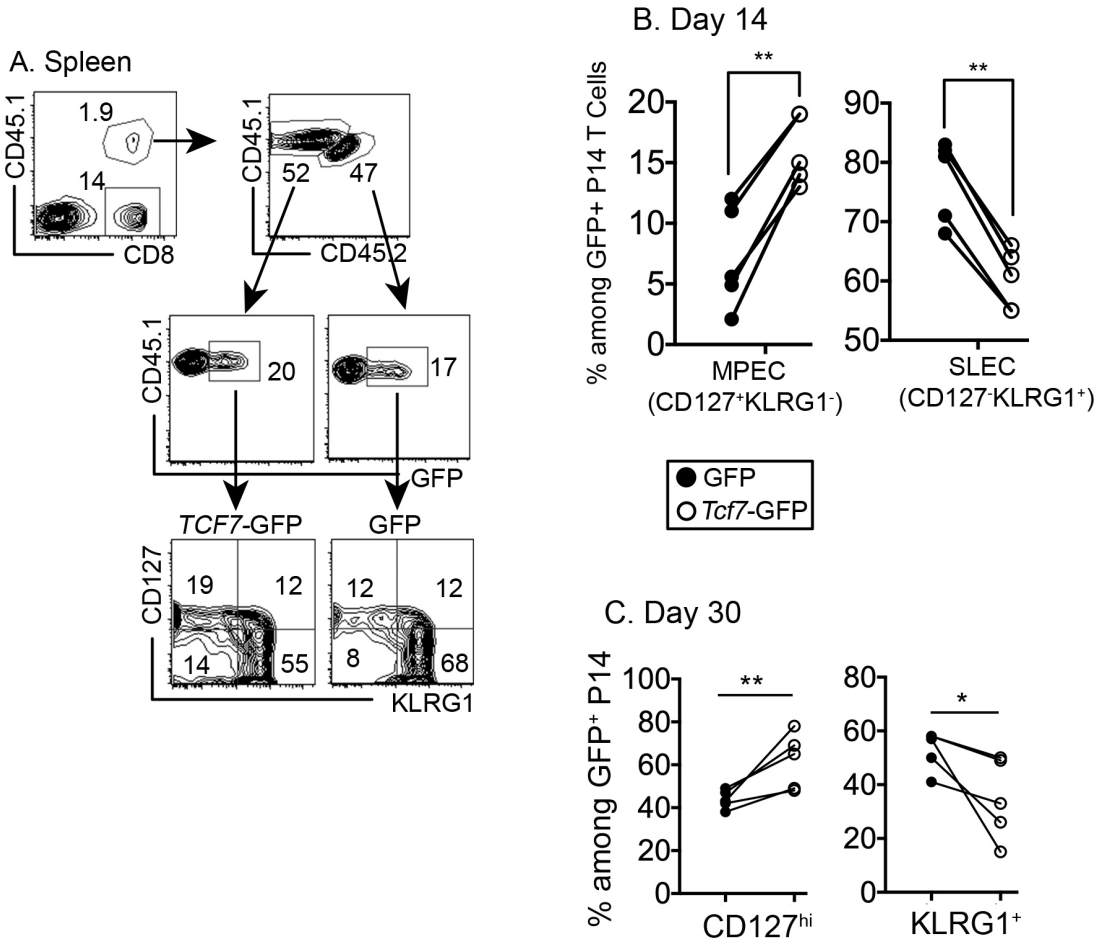

Figure S7. Overexpression of Tcf-1 promotes memory precursor differentiation in the spleen, Related to Figure 6. Similar experimental setup to **Figure 6**. FACS gating strategy is shown in (**A**). (B) Day 14 or (**C**) day 30 post infection, the percentage of KLRG1$^-$CD127$^+$ cells (**left**) and KLRG1$^+$CD127$^-$ cells (**right**) among GFP$^+$ P14 T cells are shown. Each pair of symbols represents the results from an individual recipient. *, $p<0.05$ and **, $p<0.01$ by paired Student *t*-test. Pooled results from 2 independent experiments are shown.

Transparent Methods

Ethics Statement.

All the animal handling and experimental procedures performed have adhered strictly to the general guidelines of Animal Welfare Act (AWA), AAALAC and IACUC. An Animal Care Protocol has been approved by UT Health San Antonio IACUC (protocol# 20150014AR, PI: Nu Zhang). All infectious agents used have been approved by UT Health San Antonio Institutional Biosafety Committee (protocol# 14-09-6080, PI: Nu Zhang).

Mice, Viruses and Bacteria.

Tgfbr2$^{f/f}$ dLck-cre mice were as described before (Zhang and Bevan, 2012, 2013). *Il18r1*$^{-/-}$ (stock no. 004131), and C57BL/6 (stock no. 000664) mice were obtained from The Jackson Laboratory and a colony of D^b-GP_{33-41} TCR transgenic (P14) mice was maintained at our specific pathogen-free animal facilities at the University of Texas Health Science Center at San Antonio (San Antonio, Texas). All recipient mice were used at 6 to 12 wk of age. Both male and female mice were used in the current project. No influence of gender or age was identified. All experiments were done in accordance with the University of Texas Health Science Center at San Antonio Institutional Animal Care and Use Committee guidelines. Mice were infected i.p. by $2x10^5$ pfu LCMV Arm. Viruses were grown and quantified as described (Ahmed et al., 1984).

Naïve T Cell Isolation and Adoptive Transfer.

Naïve $CD8^+$ T cells were isolated from pooled spleen and lymph nodes using MojoSort™ mouse CD8 T cell isolation kit (Biolegend) following manufacturer's instruction. During the first step of biotin antibody cocktail incubation, biotin-αCD44 (IM7, Biolegend) was added to label and deplete effector and memory T cells. Isolated naïve $CD8^+$ T cells were numerated, 1:1 mixed when indicated, 10^4 cells adoptively transferred into each sex-matched unmanipulated B6 recipient via an i.v. route.

Intra-vascular Labeling of $CD8^+$ T Cells.

3μg biotin-αCD8α (53-6.7, Tonbo Biosciences) was injected i.v. 5 mins before euthanasia. After lymphocyte isolation, fluorescence labeled streptavidin (Thermo Fisher) was used during surface staining to identify blood-borne $CD8^+$ T cells.

Lymphocyte Isolation from the Kidney, SG and SI-IEL.

Lymphocyte isolation procedures have been described before (Liao, 2020; Ma et al., 2017; Zhang and Bevan, 2013). Briefly, kidney and SG was minced and digested with 1mg/ml collagenase B (Roche) in RPMI 1640/2% FCS at 37°C for 45 mins with gentle shaking. Digested tissues were further mashed and washed with RPMI 1640/10% FCS. For IEL isolation, small pieces of the small intestine were stirred at 800 rpm for 20 min in HBSS buffer containing 1mM dithiothreitol and 10% FCS at 37°C. Both digested kidney and SG, and released IEL were further purified by density gradient centrifugation with PBS-balanced 44% and 67% Percoll (GE Healthcare).

Parabiosis Surgery.

Parabiosis surgery was performed according to a published protocol (Kamran et al., 2013). Briefly, mice were anesthetized and shaved along opposite lateral flanks. Skin was thoroughly cleaned. Longitudinal skin incisions were performed on the shaved sides of each mouse. The skin of the two animals was connected with 5-0 VICRYL suture. Additional 3-0 sutures were placed through the olecranon and knee joints to secure the legs.

Ex vivo Culture of Splenic Effector P14 T Cells.

Day 4.5 post LCMV Arm infection, total splenocytes containing P14 T cells were cultured in complete RPMI with 5ng/ml IL-2 (Tonbo) and one of the following stimuli: 1μg/ml GP_{33-41} (AnaSpec), 50ng/ml hTGF-β1, 20ng/ml IFN-β, 20ng/ml IL-18, 20ng/ml IL-33 and 20ng/ml TNF. All tested

cytokines were purchased from Biolegend. 12-16 hours later, the expression of IL-18R on live P14 T cells were determined by flow cytometry.

Retrovirus Transduction.

Tcf7 (p45)-GFP (MSCV vector) was a gift from Dr. Haihui Xue. Helper plasmid pCL-Eco was a gift from Dr. Inder Verma (Addgene plasmid#12371). *Tcf7*-GFP and pCL-Eco were co-transfected into 293T cells by FuGENE 6 (Promega). Retrovirus was harvested 48 hours after transfection and used freshly. Naïve P14 T cells were stimulated with 10nM GP_{33-41} peptide (AnaSpec) plus soluble 1μg/ml αCD28 (E18, Biolegend) in the presence of 5ng/ml IL-2 (eBioscience) overnight. Activated P14 T cells were spin infected with retrovirus at 3,000rpm 30°C for 1.5 hours in the presence of 8μg/ml polybrene (Sigma) and 5ng/ml IL-2. After spin infection, P14 T cells were incubated with retrovirus for another hour at 37°C. After extensive wash, $2x10^5$ P14 T cells were adoptively transferred into each B6 recipient followed by LCMV Arm infection.

RNA-seq Analysis.

Day 12 after infection, pooled kidney P14 T cells from 10-15 recipient mice were FACS sorted into $CD69^-$, $CD69^+IL\text{-}18R^{hi}$ and $CD69^+IL\text{-}18R^{lo}$ cells. Total RNA was extracted from sorted cells using a Quick-RNA Miniprep kit from Zymo Research. Sequencing library was constructed according to Illumina TruSeq Total RNA Sample Preparation Guide (RS-122-2201). Each library was barcoded and then pooled for cluster generation and sequencing run with 50bp single-end sequencing protocol on an Illumina HiSeq 3000 platform. Original RNA-seq results can be accessed by GSE111801.

Antibodies and Flow Cytometry.

For in vivo type I IFN blocking, 1mg anti-IFNAR-1 (MAR1-5A3, BioXcell) was given i.p. on day 4 and day 7 post LCMV infection. For flow cytometry, single cell suspension from spleen, kidney and gut IEL was incubated with FcR blocker (clone 2.4G2, generated in the lab). Cells were typically stained with fluorescence labeled streptavidin (Thermo Fisher), IL-18Rα (P3TUNYA, eBioscience), CD8β (H35-17.2, eBioscience), CD45.1 (A20, Tonbo), CD45.2 (104, Tonbo), CD11b (M1/70, Tonbo) and the following antibodies from BioLegend, CD127 (A7R34), KLRG1 (2F1/KLRG1), CD69 (H1.2F3), CD16/32(2.4G2), CD73 (TY/11.8), CD103 (2E7), CD90.1 (OX-7), CXCR3 (CXCR3-173), Ly6C (HK1.4), CD38 (90) and CXCR4 (L276F12). Cmah activity was determined by an anti-Neu5Gc antibody kit from Biolegend. Fixable Viability Dye eFluor 506 (eBioscience) or Ghost Dye™ Violet 510 (Tonbo) was used to identify live cells. For Tcf-1 staining, surface stained cells were treated by True-Nuclear TF Buffer Set (Biolegend) and stained with anti-Tcf-1 (C63D9, Cell Signaling). Washed and fixed samples were analyzed by BD LSRII or BD FACSCelesta, and analyzed by FlowJO (TreeStar) software.

In vivo IFN-γ Production During Reactivation.

After 30 days of LCMV infection, we re-challenged the mice with 32μg GP_{33-41} peptide/mouse (Genscript) via an i.v. route together with 250μg Brefeldin A (B6542, Sigma) in 200μl PBS 4 hours before euthanasia similar to a previous report (Sega et al., 2014). During the lymphocyte isolation procedure of kidney, 5μg/ml Brefeldin A was added to the digestion buffer and density gradient centrifugation buffer. Freshly isolated lymphocytes were surface stained, fixed, permeablized and intracellular stained by anti-IFN-γ antibody (XMG1.2, Biolegend) and anti-granzyme B (NGZB, Invitrogen).

Ex vivo Stimulation to Detect Cytokine Production.

Fresh isolated lymphocytes from various tissues were cultured in complete RPMI in the presence of Golgi STOP with or without different stimuli for 4 hours. Stimuli used in current study include 1μM GP_{33-41}, 20ng/ml IL-12+20ng/ml IL-18 or 20ng/ml IL-12+20ng/ml IL-18+20ng/ml IL-15+ 20ng/ml IFN-α. All recombinant mouse cytokines were purchased from Biolegend. Stimulated cells were surface stained, fixed, permeablized and intracellular stained by anti-IFN-γ antibody (XMG1.2, Biolegend) and anti-TNF antibody (MP6-XT22, Biolegend). Ghost Dye™ Violet 510 (Tonbo) was

used to identify live cells. Washed samples were analyzed by BD FACSCelesta, and analyzed by FlowJO (TreeStar) software.

Statistic Analysis.

P value was calculated by two-tail paired or unpaired Student *t*-test, One-way ANOVA using Prism 7 software.

Supplemental References

Ahmed, R., Salmi, A., Butler, L.D., Chiller, J.M., and Oldstone, M.B. (1984). Selection of genetic variants of lymphocytic choriomeningitis virus in spleens of persistently infected mice. Role in suppression of cytotoxic T lymphocyte response and viral persistence. J. Exp. Med. *160*, 521-540.

Kamran, P., Sereti, K.I., Zhao, P., Ali, S.R., Weissman, I.L., and Ardehali, R. (2013). Parabiosis in mice: a detailed protocol. J Vis Exp.

Liao, W., Ma, C., Zhang, N. (2020). Isolation of Mouse Kidney-Resident CD8+ T cells for Flow Cytometry Analysis. J. Vis. Exp., e61590.

Ma, C., Mishra, S., Demel, E.L., Liu, Y., and Zhang, N. (2017). TGF-beta Controls the Formation of Kidney-Resident T Cells via Promoting Effector T Cell Extravasation. J. Immunol. *198*, 749-756.
Sega, E.I., Leveson-Gower, D.B., Florek, M., Schneidawind, D., Luong, R.H., and Negrin, R.S. (2014). Role of lymphocyte activation gene-3 (Lag-3) in conventional and regulatory T cell function in allogeneic transplantation. PLoS One *9*, e86551.

Zhang, N., and Bevan, M.J. (2012). TGF-beta signaling to T cells inhibits autoimmunity during lymphopenia-driven proliferation. Nat. Immunol. *13*, 667-673.

Zhang, N., and Bevan, M.J. (2013). Transforming growth factor-beta signaling controls the formation and maintenance of gut-resident memory T cells by regulating migration and retention. Immunity *39*, 687-696.